Supplementary Information

Peptide nano-blanket impedes fibroblasts activation and subsequent formation of pre-metastatic niche

Yi Zhou[1], Peng Ke[1 4], Yiyi Xia[1], Honghui Wu[1], Zhentao Zhang[1], Haiqing Zhong[1], Qi Dai[1 5], Tiantian Wang[1], Mengting Lin[1], Yaosheng Li[1], Xinchi Jiang[1], Qiyao Yang[1 5], Yiying Lu[1], Xincheng Zhong[1], Min Han[1 2 3*], Jianqing Gao[1 2 3*]

[1] Institute of Pharmaceutics, Zhejiang Province Key Laboratory of Anti-Cancer Drug Research, College of Pharmaceutical Sciences, Zhejiang University, Hangzhou 310058, P.R. China

[2] Cancer Center of Zhejiang University, Zhejiang University, Hangzhou 310058, P.R. China.

[3] Hangzhou Institute of Innovative Medicine, Zhejiang University, Hangzhou 310058, P.R. China.

[4] Shengli Clinical Medical College of Fujian Medical University, Fuzhou, 350001, China.

[5] Department of Radiation Oncology, Key Laboratory of Cancer Prevention and Intervention, The Second Affiliated Hospital, College of Medicine, Zhejiang University, Hangzhou 310058, China.

* Corresponding author: hanmin@zju.edu.cn (M. H.); gaojianqing@zju.edu.cn (J. G.)

Contents

Supplementary Methods **4**

Mass spectrometry and MS/MS 4

Circular dichroism analysis 4

Peptide self-assembly of TPE-FG8 5

Peptides inhibiting MLF stimulation on the proliferation of bEnd3 cells 5

Proliferation and migration of tumor cells with FR17 treatment 5

Supplementary Figures 7

Figure S1. Mass spectrometry of FR17 and sFD17 7

Figure S2. Tandem mass spectrometry of FR17 and sFD17 8

Figure S3. Enzyme-activated assembly of FR17 and sFD17 9

Figure S4. Self-assembly of FFKY and FG8 10

Figure S5. The pathological process in the lung of MCM-induced PMN model *in vivo* 11

Figure S6. Immune cell population analysis during the pathological process in the lung of MCM-induced PMN model *in vivo* 12

Figure S7. Flow cytometry gating strategy for the analysis of immune cell population in pulmonary PMN 13

Figure S8. MCM-induced PMN formation aggravate metastasis *in vivo* 14

Figure S9. FR17 administration inhibit extracellular matrix remodeling in pulmonary PMN 15

Figure S10. FR17 protects fibroblasts from being irritated by MCM to prevent the disrupting endothelial cell-cell connection and cell proliferation 16

Figure S11. FR17 administration down-regulates matrix metalloproteinase in pulmonary PMN 17

Figure S12. FR17 administration prevents MDSC recruitment to pulmonary PMN by influencing the extracellular matrix remodeling 18

Figure S13. Flow cytometry gating strategy for the analysis of $CD11b^{+}Ly6G^{+}$ MDSC recruited to the pulmonary PMN 19

Figure S14. The alleviation of PMN development by FR17 administration correlate to the cell pathway of myeloid leukocyte migration and the activation of immune response 20

Figure S15. Effect of FR17 treatment on the proliferation of tumor cells and MLF, and on tumor cell's migration.....21
Figure S16. Preliminary safety evaluation of peptide administration on lung metastasis model with MCM-induced PMN *in vivo*..... 22
Figure S17. Preliminary safety evaluation of peptide administration by the Hematoxylin & Eosin staining of major organs..... 23
Figure S18. Tumor volume curve of the recurrent tumor on the back of mice post-surgery 24

Supplementary Methods

Mass spectrometry and MS/MS： Mass spectrometry was conducted using AB Triple TOF 5600plus System (AB SCIEX, Framingham, USA). File was created with the software version: Analyst TF 1.6. Syringe Pump Flow rate was set as 10 μL/min. The optimal MS conditions were set as followed: Positive ion mode: source voltage was set to + 5.5 kV, and the source temperature was set to normal atmospheric temperature. The pressure of Gas 1 (Air) and Gas 2 (Air) were set as 25 psi. The pressure of Curtain Gas (N2) was set as 25 psi. Maximum allowed error was set at ± 5 ppm. Declustering potential (DP) was set as 100 V; collision energy (CE) was set as 10 V.

For MS/MS acquisition, the parameters were almost the same except that the collision energy (CE) was set at 45 ± 15 V for the first time and 50 ± 10 V for the second time, ion release delay (IRD) was set at 67, ion release width (IRW) was set at 25. The scan range of m/z of precursor ion was set as 100-2,000 Da and product ion as 100-2,000 Da. The exact mass calibration was performed automatically before each analysis using the Automated Calibration Delivery System. The data acquisition and analysis were performed by PeakView software (version 1.2, AB Sciex, USA).

Circular dichroism analysis. For circular dichroism analysis, FR17 or sFD17 cultivated with type IV collagenase at the working concentration of 0.5 mg/mL in HBS buffer for 24 h was dialyzed for 24 h in 300 Da dialysis bag in DD-water. Data were analyzed using CD Deconvolution.

Peptide self-assembly of TPE-FG8. TPE modification was realized via aldimine condensation reaction between carboxyl group on TPE and amino group from the N-terminal of Phe of peptide, *i.e.* FFKY or FG8 or FR17. For aggregation-induced luminescence effect, TPE modified peptides were firstly dissolved in methanol as stock solution and then diluted with 99 volumes of water to achieve self-assembly. The emission spectrum of final suspensions was detected using fluorescence spectrophotometer under the excitation wavelength at 405 nm. The microstructure of the assemblies was observed by FEI Tecnai G2 spirit transmission electron microscope.

Peptides inhibiting MLF stimulation on the proliferation of bEnd3 cells. bEnd3 cells in rapid proliferation were plated in 96-well plates at proper density and cultured overnight. Former media were removed and replaced by conditional FCM, which was obtained from MLFs stimulated by MCM with or without the treatment of different peptides (TP5, sFD17, FR17 at the concentration of 100 μM) as illustrated above. Cell cultivated with normal FCM was set up as control. Cell proliferation was measured after incubated for 48 h using a Cell Counting Kit-8 (CCK8) assay (Cat. 13E02A60, Boster BioTech., China), $OD_{450\ nm}$ was read by a multiwell plate reader (ELX800, Biotek, USA).

Proliferation and migration of tumor cells with FR17 treatment. B16F10 cells in rapid

proliferation were plated in 96-well plates at proper density and cultured overnight. FR17 at various concentrations (0-1000 μM) was cultivated with B16F10 for 24 or 72 h. Cell proliferation was measured by CCK8 assay (Cat. 13E02A60, Boster BioTech., China) as formerly introduced. Cell viability was normalized by the reads from untreated wells. For migration assay, tumor cells were plated in Culture-Inserts (2 Well, Ibidi, Germany) at proper density and grow to confluence overnight. Culture-Inserts as well as the former medium were gently removed. And the cells were cultivated with low, medium and high concentration of FR17 at 40, 200, 1000 μM in triplicate. Cell cultivated with fresh complete medium was set up as control. Pictures of the cell scratches were taken under the microscope at 0, 6, 12, 24 h respectively. After incubated for 24 h, cells were fixed and stained with crystal violet. Images were analyzed with ImageJ.

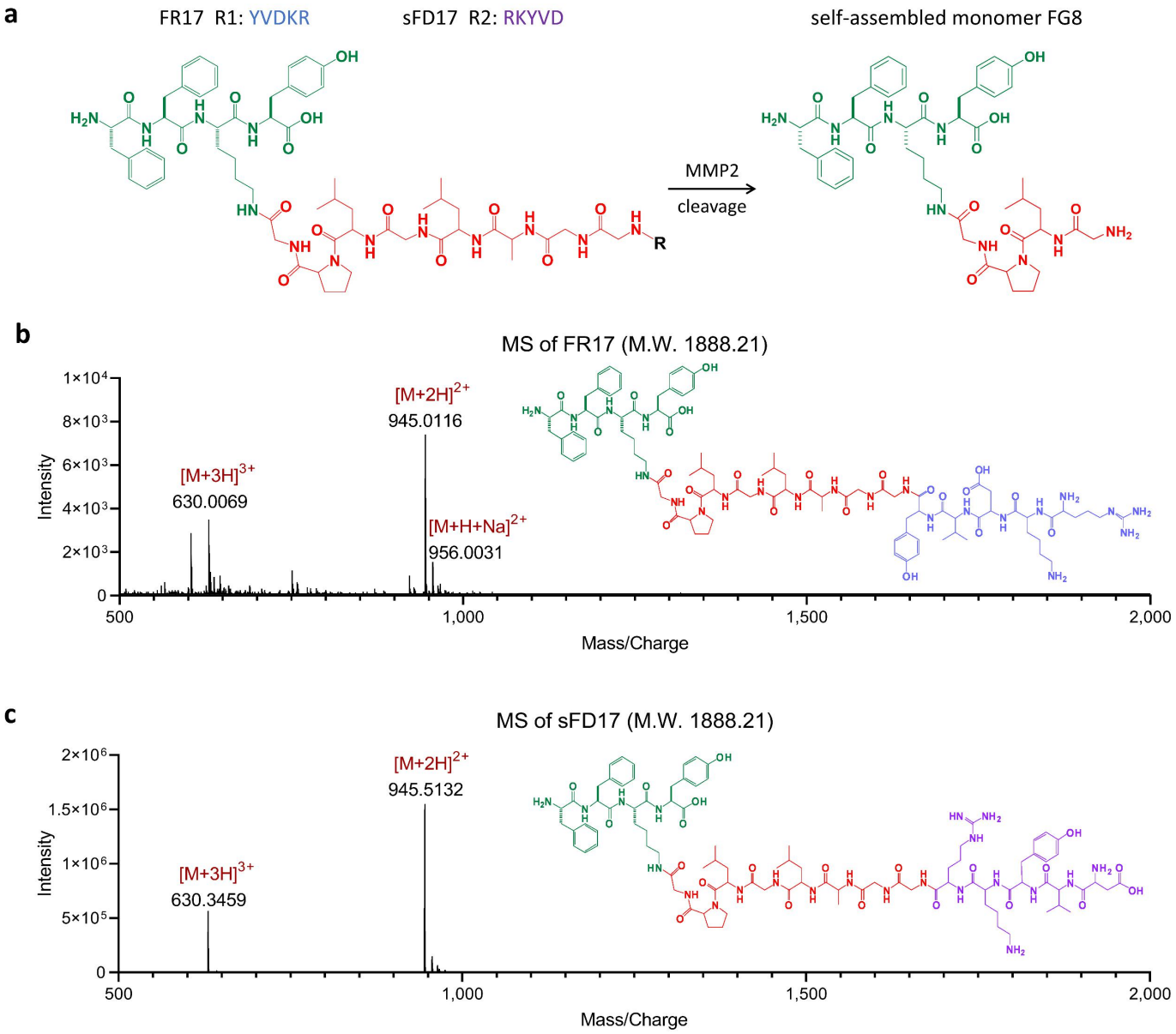

1 **Supplementary Figure 1. Mass spectrometry of FR17 and sFD17. a**, Schematic enzyme

2 cleavage of FR17 or sFD17 to release the self-assembled monomer FG8. **b**, Mass spectrum and

3 the molecular structure of FR17 (MW. 1888.12). **c**, Mass spectrum and the molecular structure of

4 sFD17 (MW. 1888.12).

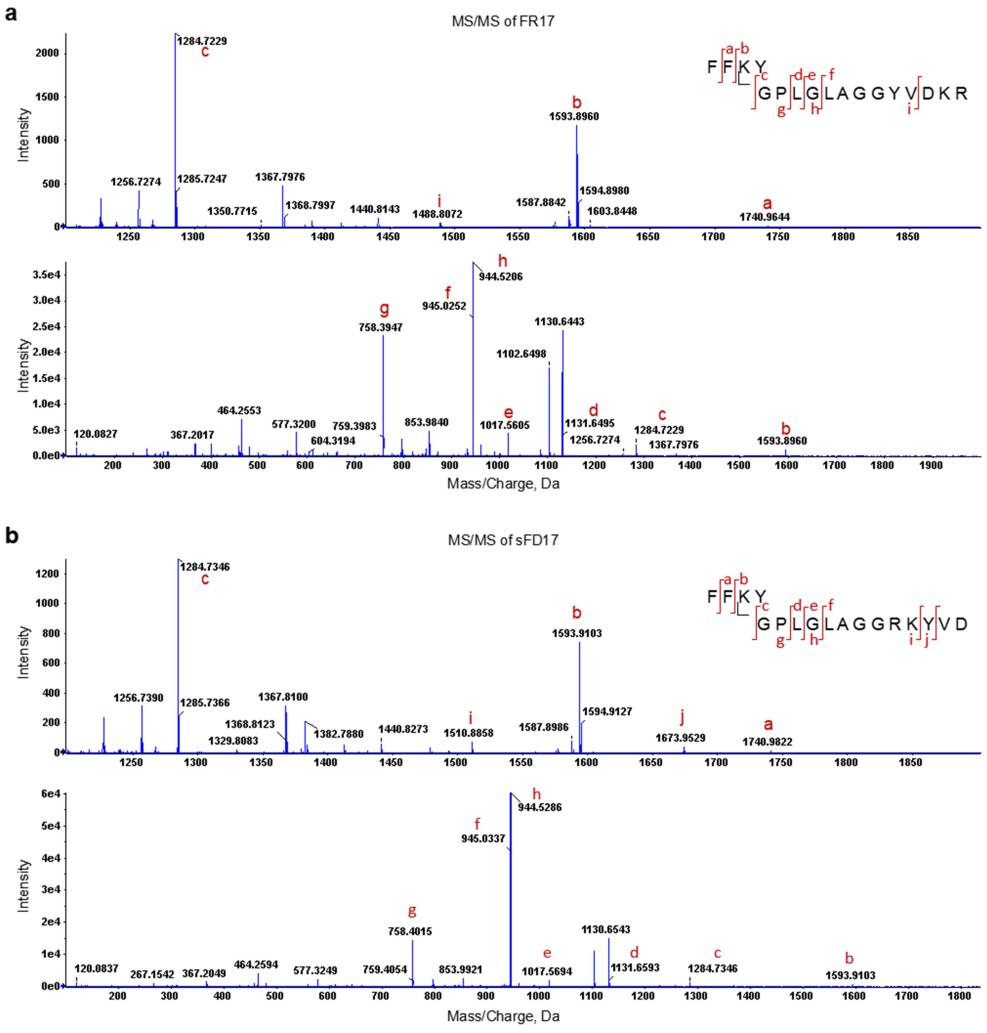

Supplementary Figure 2. Tandem mass spectrometry of FR17 and sFD17. a, MS/MS of FR17. The tandem mass spectrometry on the upper row of (a) was obtained as CE set at 50 ± 10 V. The tandem mass spectrometry on the lower row of (a) was obtained as CE set at 45 ± 15 V. The red characters a-i represent for different peptide fragments labeled on the top left corner. **b**, MS/MS of sFD17. The tandem mass spectrometry on the upper row of (b) was obtained as CE set at 50 ± 10 V. The tandem mass spectrometry on the upper row of (b) was obtained as CE set at 45 ± 15 V. The red characters a-j represent for different peptide fragments labeled on the top left corner.

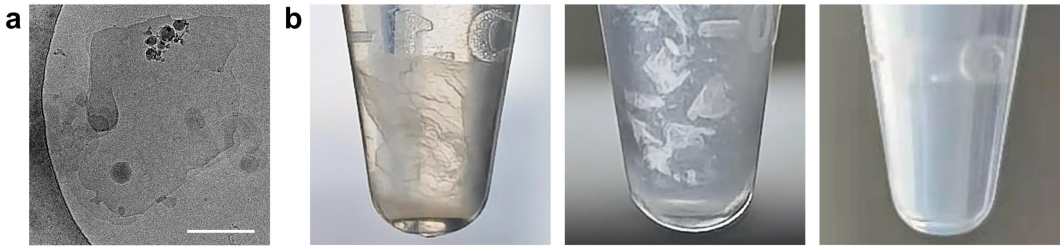

c

190-260 nm	FR17	FR17+enzyme	sFD17	sFD17+enzyme
Helix	6.50%	6.20%	6.20%	6.20%
Antiparallel	36.80%	48.70%	40.00%	48.80%
Parallel	3.30%	3.70%	3.40%	3.70%
Beta-Turn	20.30%	16.70%	19.10%	16.70%
Rndm. Coil	33.80%	29.10%	32.50%	29.10%

Supplementary Figure 3. Enzyme-activated assembly of FR17 and sFD17. a, Cryo-TEM image of the peptide nano-blanket assembled by FR17 treated with MMP2 for 24 h. Scale bar = 200 nm. **b**, Macroscopic images of the thin layer formed by FR17 treated with enzyme and let stand for 72 h. The soft thin layer broke into pieces after gently shaking and dispersed into nanoscale fragment after sharply shaking. **c**, Circular dichroism analysis of peptide and the enzyme-activated assembled peptide nano-blanket by FR17 and sFD17 being treated with enzyme for 24 h.

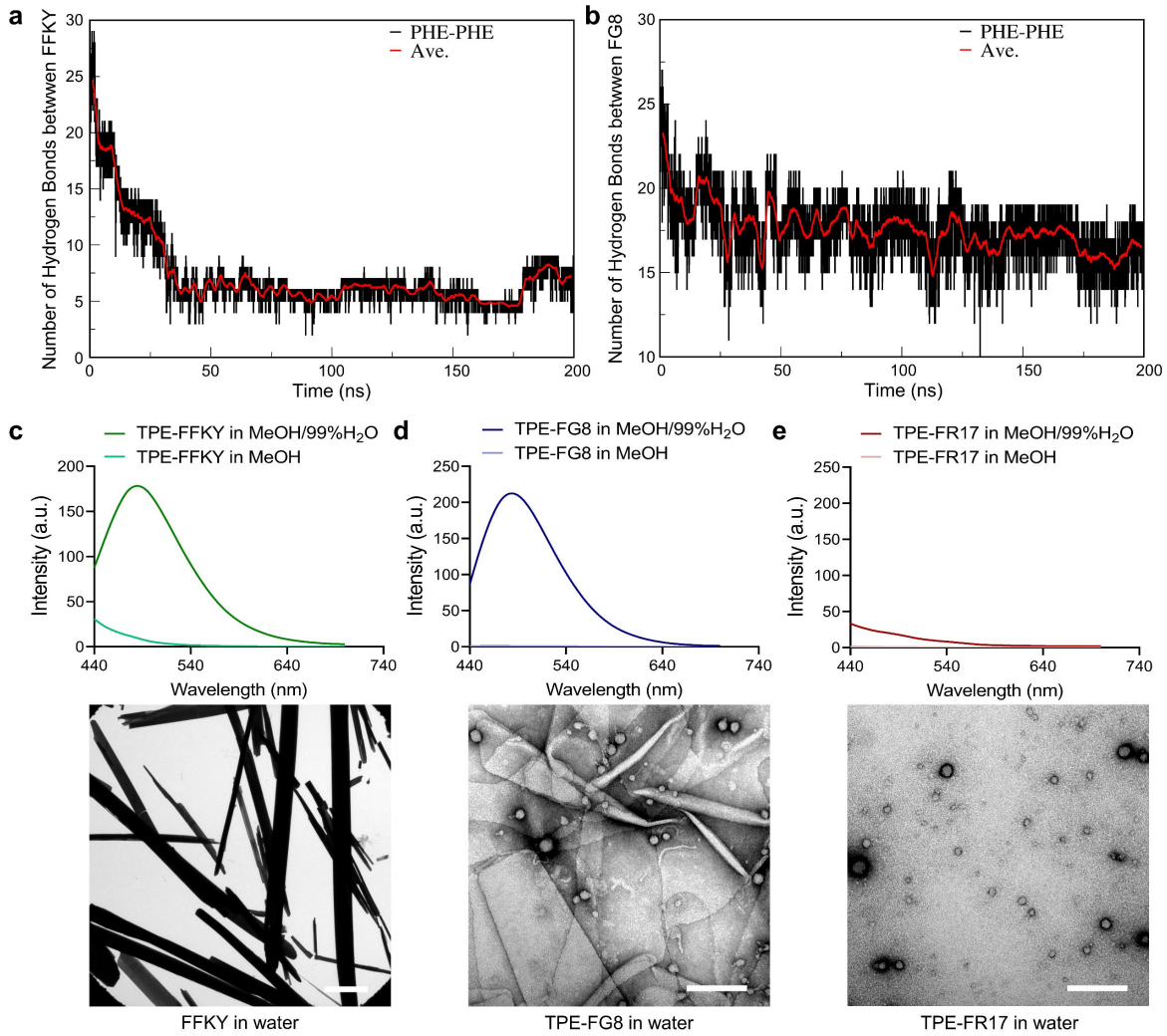

Supplementary Figure 4. Self-assembly of FFKY and FG8. a-b, Hydrogen Bonds formed in FFKY or FG8 system as a function of time. **c,** Fluorescence spectra of the TPE-FFKY in methanol (dissolved) and water at methanol fraction of 1% (assembled as illustrated in the TEM image below) excited by 405 nm. Scale bar = 10 μm. **d,** Fluorescence spectra of the TPE-FG8 in methanol (dissolved) and water at methanol fraction of 1% (assembled as illustrated in the TEM image below) excited by 405 nm. Scale bar = 200 nm. **e,** Fluorescence spectra of the TPE-FR17 in methanol and water at methanol fraction of 1% (dispersed as illustrated in the TEM image below). Scale bar = 200 nm.

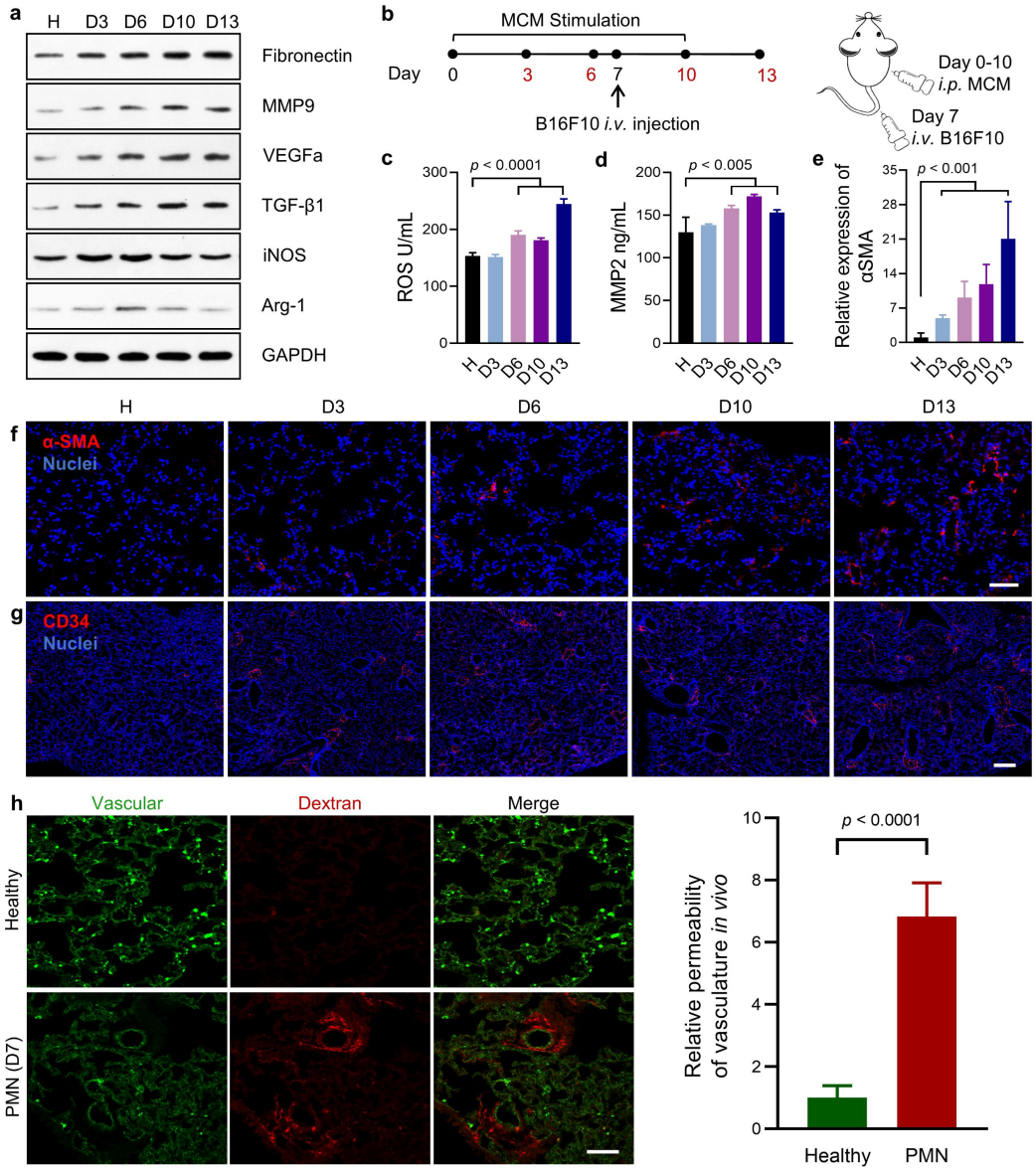

Supplementary Figure 5. The pathological process in the lung of MCM-induced PMN model *in vivo*. **a**, The alteration of Fibronectin, MMP9, VEGFa, TGF-β1, iNOS and Arg-1 expression level in the lung during the development of PMN. **b**, The timeline of MCM-induced PMN model. **c & d**, ROS and MMP2 level in the lung during the development of PMN. Data is presented as mean ± SD. n = 4. **e & f,** Representative immunofluorescence images of the lung during the PMN development showing activation of fibroblasts indicated by αSMA+ labeling. Scale bar = 50 μm. Semi-quantification was gained from six random fields via ImageJ. Two-tail *t*-test was performed

for statistical evaluation compared to Healthy group. **g**, Representative immunofluorescence images of the lung during the PMN development showing angiogenesis indicated by $CD34^+$ labeling. Scale bar = 250 μm. “H”, “D3”, “D6”, “D10”, “D13” are the abbreviations of “Healthy”, “Day 3”, “Day 6”, “Day 10”, “Day 13” in the figure labeling. **h**, Vascular permeability of the pulmonary PMN on Day 7. Scale bar = 50 μm. Data is presented as mean ± SD. n = 3 biologically independent mice. One-way ANOVA followed by Tukey’s multiple comparisons test was performed for statistical evaluation.

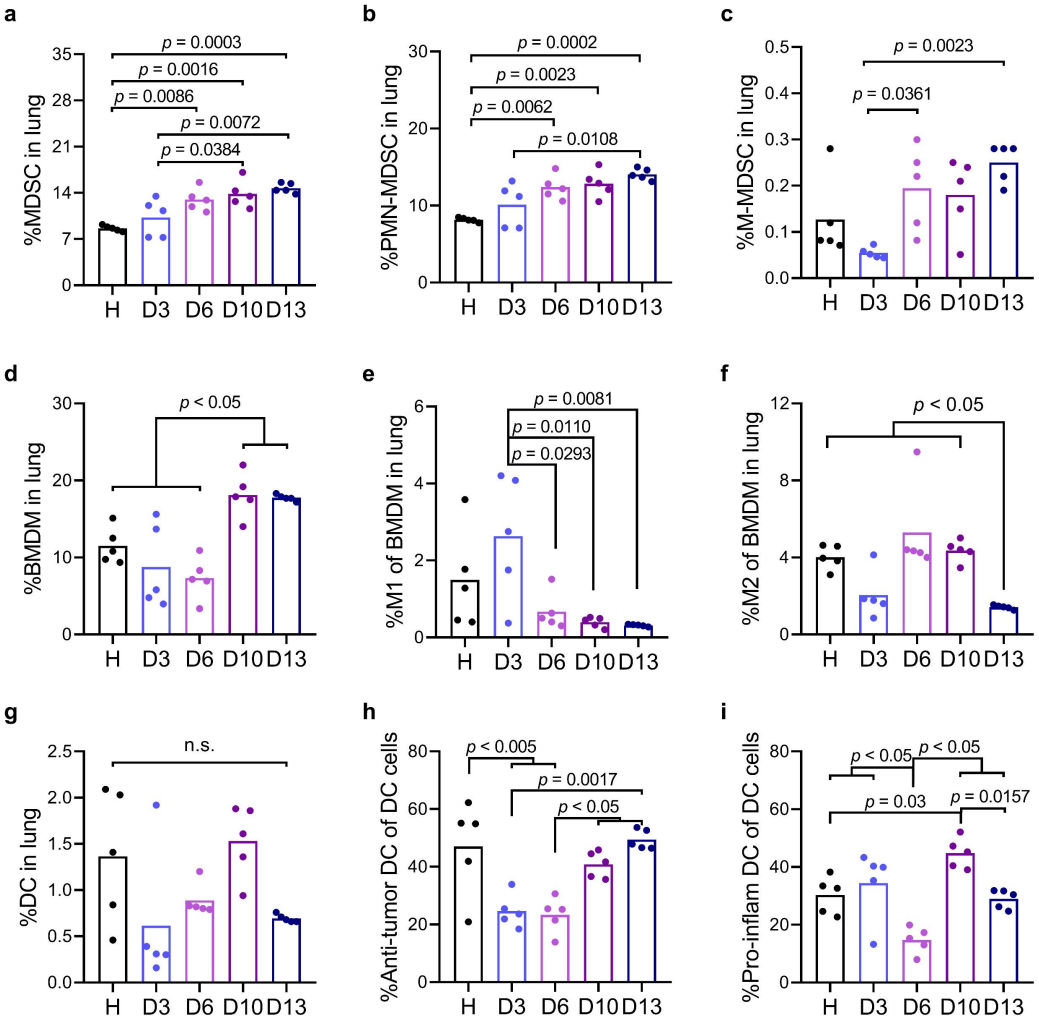

Supplementary Figure 6. Immune cell population analysis during the pathological process in the lung of MCM-induced PMN model *in vivo*. **a**, MDSC recruited to the lung; **b**, and the

alteration of the $CD11b^{+}Ly6g^{+}Ly6c^{int}$ cell population PMN-MDSC subtype; **c**, as well as the $CD11b^{+}Ly6g^{-}Ly6c^{+}$ subtype M-MDSC during the development of PMN. **d**, BMDM cells recruited to the lung; **e**, and its sub phenotype M1; **f**, and M2 along with the development of PMN. **g**, Dendritic cell (DC) population in the lung; **h**, and its sub phenotype $CD103^{+}$ DC, *i.e.* anti-tumor DC; **i**, and $CD11b^{+}$ DC, *i.e.* pro-inflame DC along with the development of PMN. "H", "D3", "D6", "D10", "D13" are the abbreviations of "Healthy", "Day 3", "Day 6", "Day 10", "Day 13" in the figure labeling. Data is presented as mean ± SD. n = 5 biologically independent mice. One-way ANOVA followed by Tukey's multiple comparisons test was performed for data analysis.

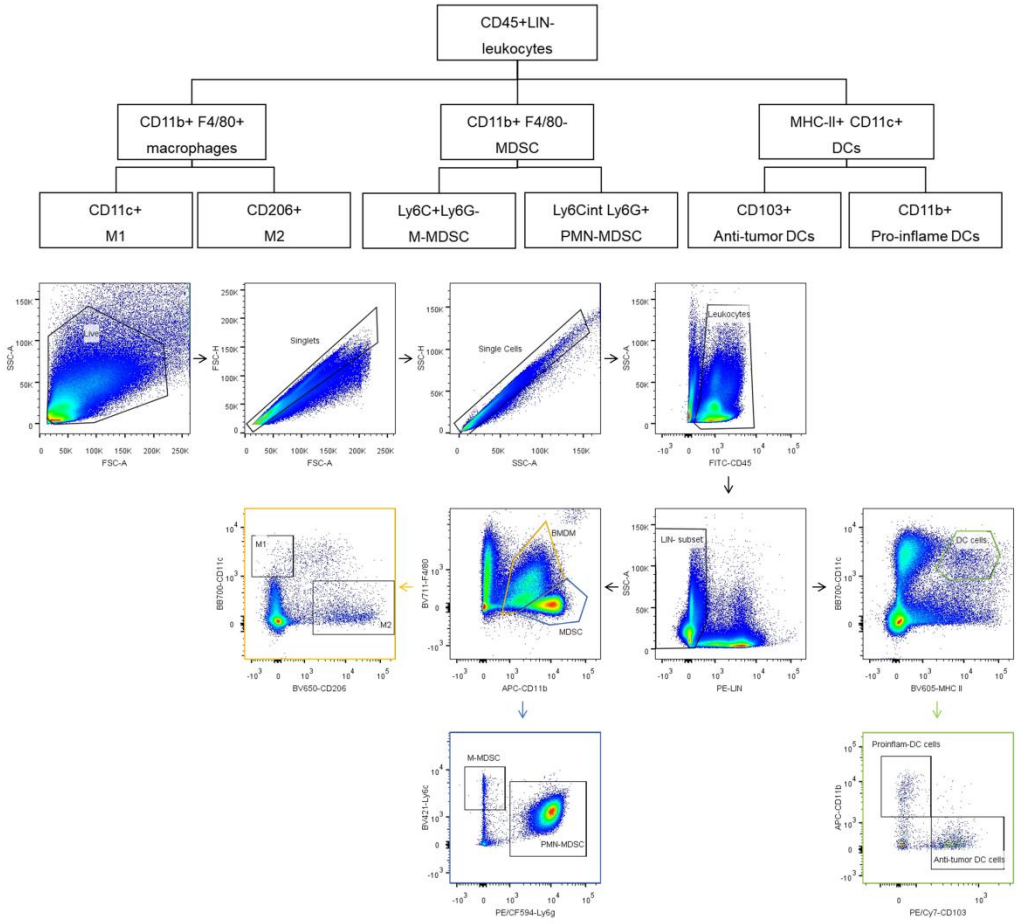

Supplementary Figure 7. Flow cytometry gating strategy for the analysis of immune cell

population in pulmonary PMN.

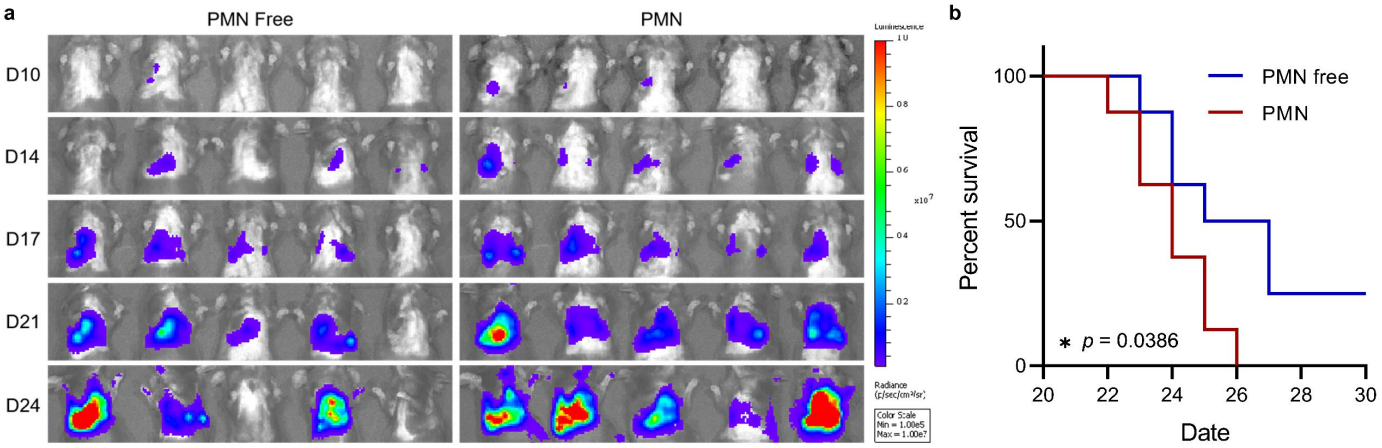

Supplementary Figure 8. MCM-induced PMN formation aggravated metastasis *in vivo*. a, *In* *vivo* bioluminescent images of the lungs of mice with or without MCM-induced PMN (n = 5). **b**, Survival curves of the lung metastatic mice with or without PMN in 30 days (n = 8). Logrank (Mantel-Cox test) was performed for curve comparison.

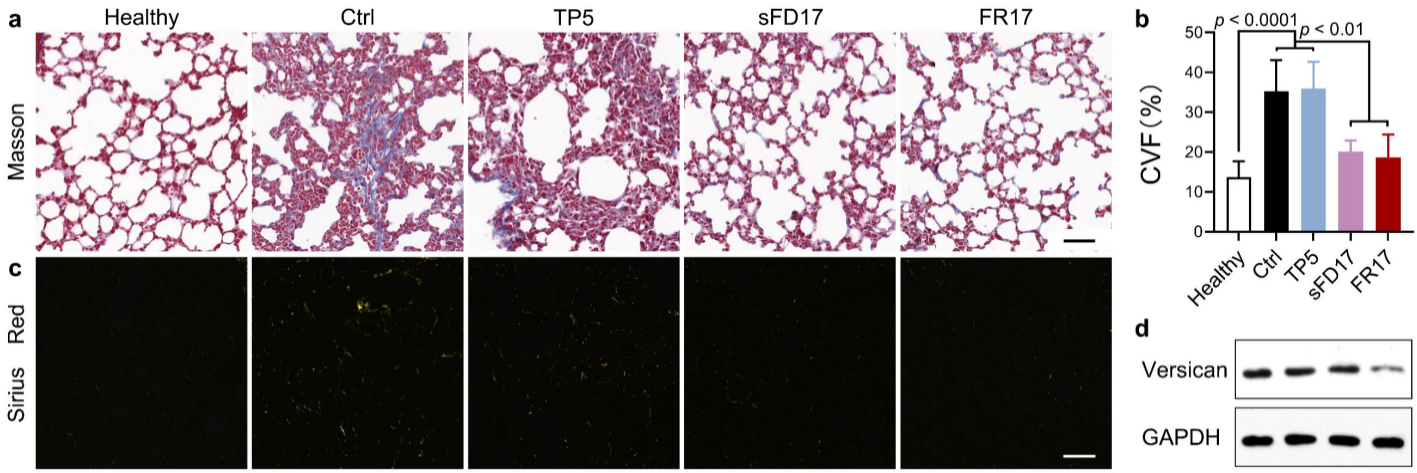

Supplementary Figure 9. FR17 administration inhibited extracellular matrix remodeling in pulmonary PMN. a, b, Representative images and semi-quantification of collagen deposition in the lung harvested from the model mice administrated with different peptides by Masson staining. Scale bar = 50 μm. Collagen volume fraction (CVF) was calculated by normalizing the blue collagen area to the total tissue area. Data is presented as mean ± SD. n = 5. One-way ANOVA followed by Tukey's multiple comparisons test was employed for data analysis. **c**, Representative images of the Sirius Red Staining sections of the lung harvested from the model mice administrated with different peptides on Day 10 taken by polarizing microscope to show the deposited collagen is mainly collagen fiber IV. Scale bar = 50 μm. **d**, Expression of versican in the lung harvested from the model mice administrated with different peptides on Day 10.

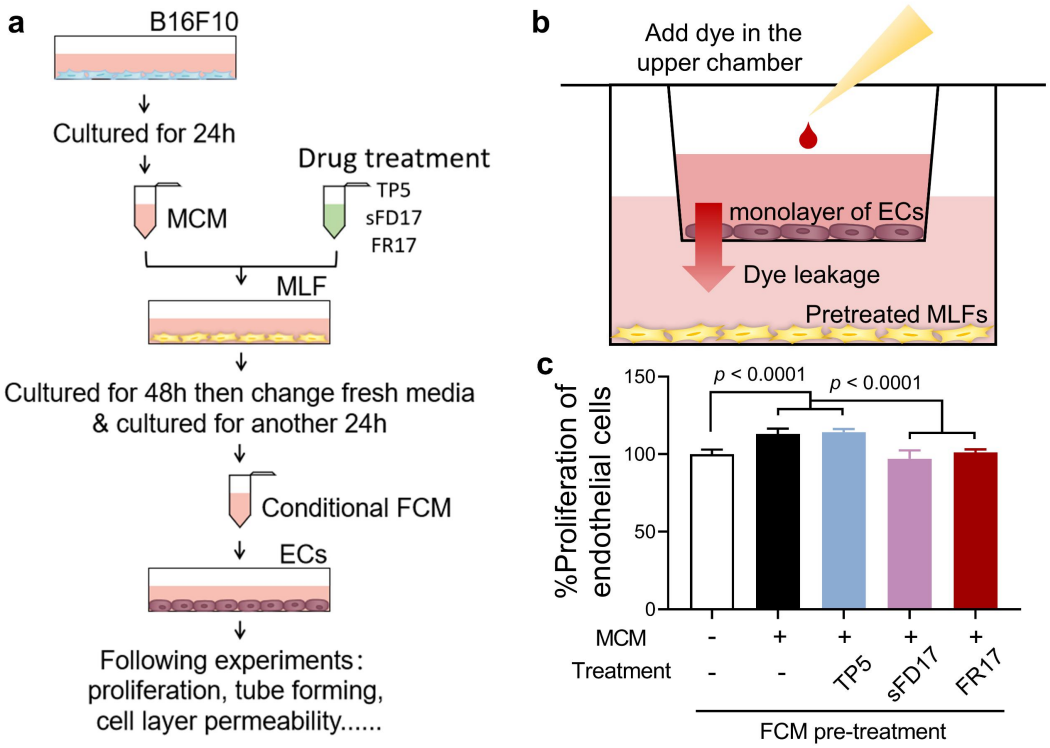

1

2 **Supplementary Figure 10. FR17 protected fibroblasts from being irritated by MCM to**

3 **prevent the disrupting endothelial cell-cell connection and cell proliferation. a**, The

4 experimental procedure to obtain the conditional FCM after MCM stimulation and the peptide

5 treatment on MLF *in vitro* for further experiments on endothelial cells. **b**, Schematic illustration of

6 the transwell permeability assay. **c**, Proliferation of the endothelial cells cultivated with

7 conditional FCM. Data is presented as mean ± SD. n = 6. One-way ANOVA followed by Tukey's

8 multiple comparisons test was employed for data analysis.

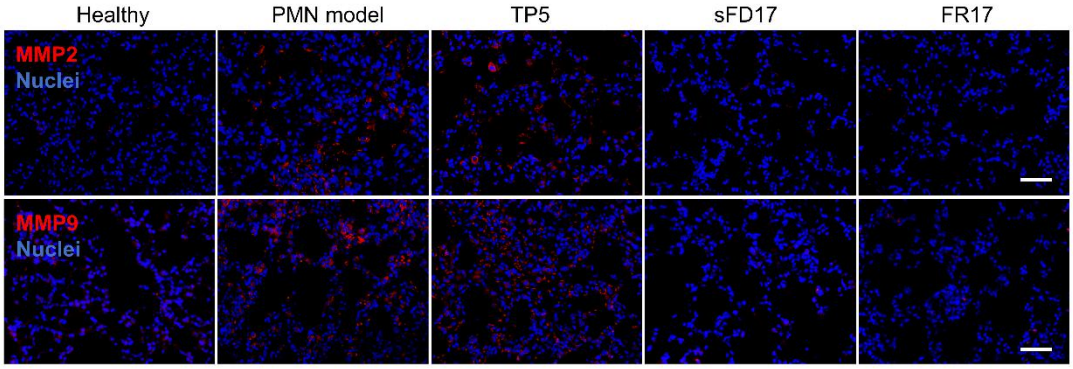

Supplementary Figure 11. FR17 administration down-regulated matrix metalloproteinase in pulmonary PMN. Representative images of MMP2 and MMP9 in the lung harvested from the PMN model mice administrated with different peptides (n = 3). Scale bar = 50 μm.

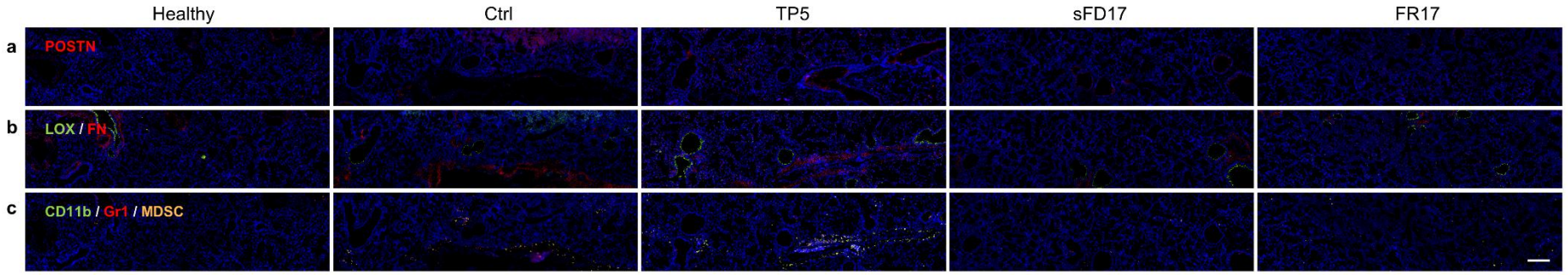

Supplementary Figure 12. FR17 administration prevented MDSC recruitment to pulmonary PMN by influencing the extracellular matrix remodeling. Images under low magnification ratio of the serial sections of the lungs harvested from the model mice treated with different peptides were taken. Serial sections show the co-location and distribution of **a**, periostin (POSTN); **b**, lysyl oxidase (LOX) and Fibronectin (FN); **c**, $CD11b^{+}Gr1^{+}$ MDSC. Scale bar = 200 μm.

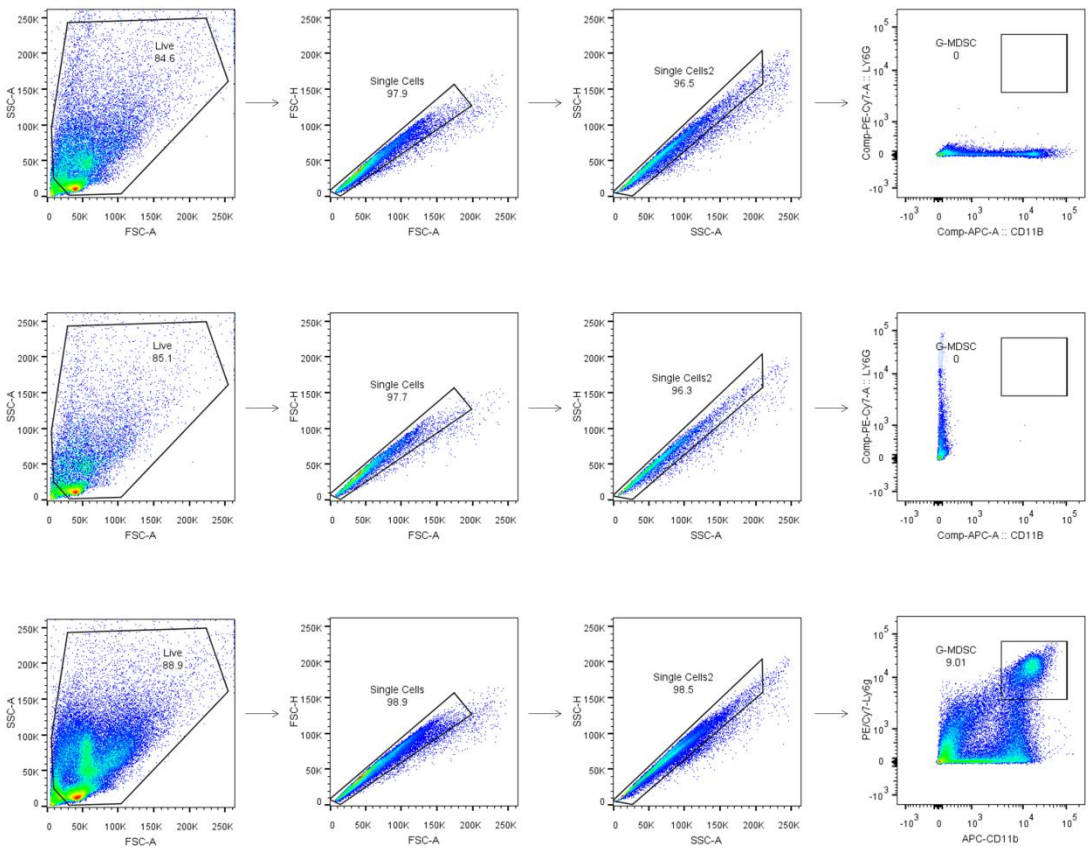

Supplementary Figure 13. Flow cytometry gating strategy for the analysis of $CD11b^{+}Ly6g^{+}$ MDSC recruited to the pulmonary PMN.

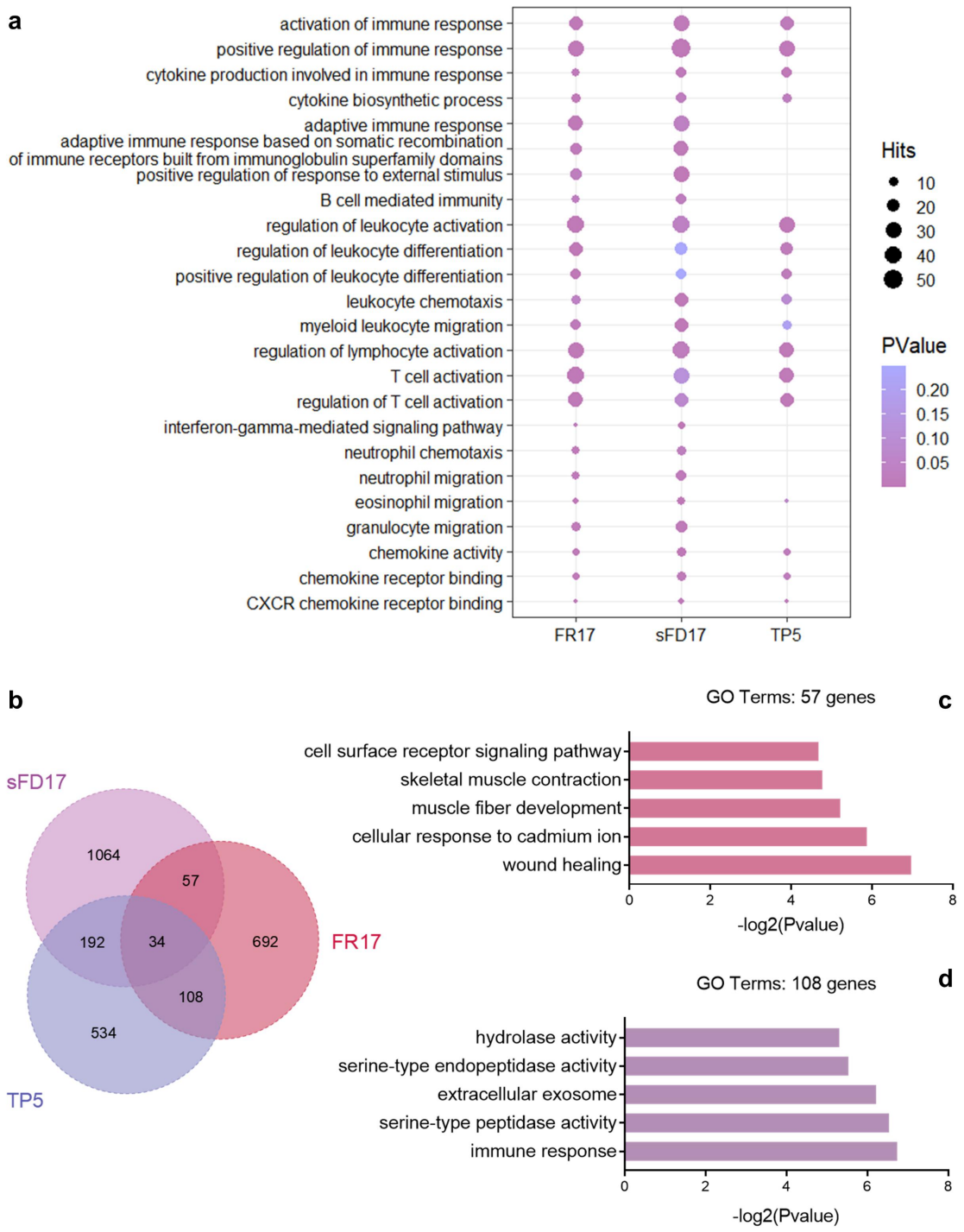

Supplementary Figure 14. The alleviation of PMN development by FR17 administration could be correlated to the cell pathway of myeloid leukocyte migration and the activation of immune response. a, GO enrichment analysis of $CD11b^{+}Ly6g^{+}$ MDSC sorted from different treatment groups on Day 10. RNA preparations were extracted from $CD11b^{+}Ly6g^{+}$ MDSCs sorted

from lungs pooled from 10–12 mice per sample. The size of the dots corresponds to the number of genes per pathway, and the color indicates *p*-value. **b**, Venn diagram of the data gained from mRNA sequencing of $CD11b^{+}Ly6g^{+}$ MDSC sorted from different treated mice. Numbers of mRNA whose expressions altered and had significance with the control group are shown in the blue, purple and red regions respectively. (Significance was determined as $p < 0.05$) **c**, GO Enrichment analysis of the 57 mRNA regulated by the PNB self-assembly (*i.e.*, the overlapping alteration in sFD17 and FR17 treated groups while excluding TP5 effect). **d**, GO Enrichment analysis of the 108 mRNA regulated by the amino acid sequence of TP5 (*i.e.*, the overlapping alteration in TP5 and FR17 treated groups while excluding sFD17 effect).

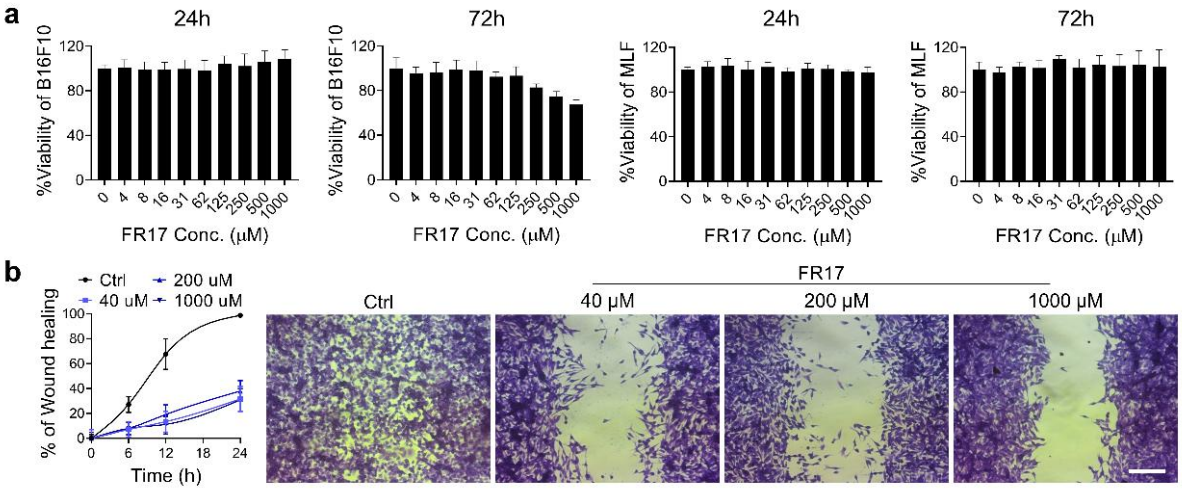

Supplementary Figure 15. Effect of FR17 treatment on the proliferation of tumor cells and MLF, and on tumor cell's migration. a, Proliferation of B16F10 and MLF treated with FR17 at different concentrations for 24 h or 72 h. Data is presented as mean ± SD. n = 6. **b**, Migration of B16F10 when treated with FR17 at different concentrations for 24 h. Data is presented as mean ± SD. n = 3. Scale bar = 200 μm.

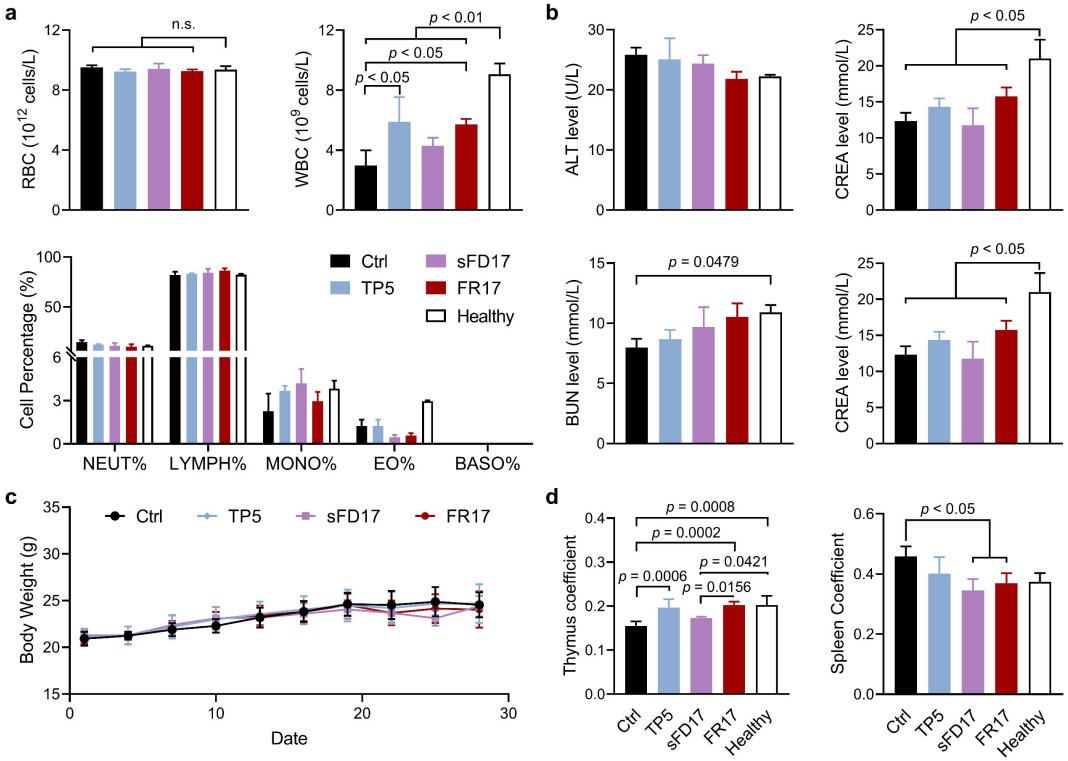

Supplementary Figure 16. Preliminary safety evaluation of peptide administration on lung metastasis model with MCM-induced PMN *in vivo*. a, Complete blood count conducted on the peripheral blood. **b**, Hepatic and renal function reflected by alanine aminotransferase (ALT), aspartate aminotransferase (AST), blood urea nitrogen (BUN) and serum creatinine (CREA). Blood samples were collected on Day 20 from the lung metastasis model mice administrated with different peptides. Data is presented as mean ± SD. n = 4 biologically independent mice for peptide treated groups and 3 for control and healthy groups. **c**, Weight curve of the lung metastasis model mice administrated with different peptides. Data is presented as mean ± SD. n = 7. **d**, Thymus coefficient and spleen coefficient of the lung metastasis model mice administrated with different peptides at the end of the experiment. The organ coefficient was calculated by normalizing the organ's weight to the body weight. Data is presented as mean ± SD. n = 5. One-way ANOVA followed by Tukey's multiple comparisons test was employed for data analysis.

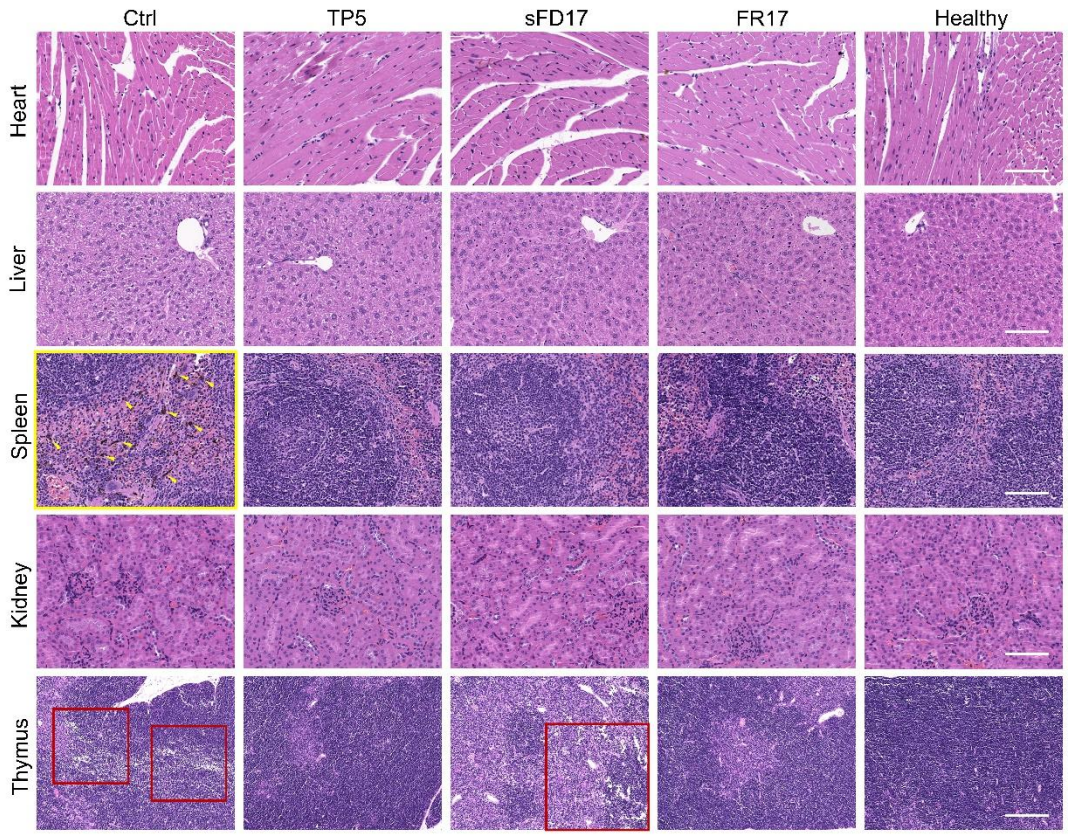

Supplementary Figure 17. Preliminary safety evaluation of peptide administration by the Hematoxylin & Eosin staining of major organs. The yellow arrows indicate the infiltrated B16F10 cells into the spleen of the control mice. The red boxes show slightly atrophied of the thymuses with the unoccupied zones. Scale bar = 100 μm for heart, liver, spleen and kidney sections. Scale bar = 200 μm for Thymus sections.

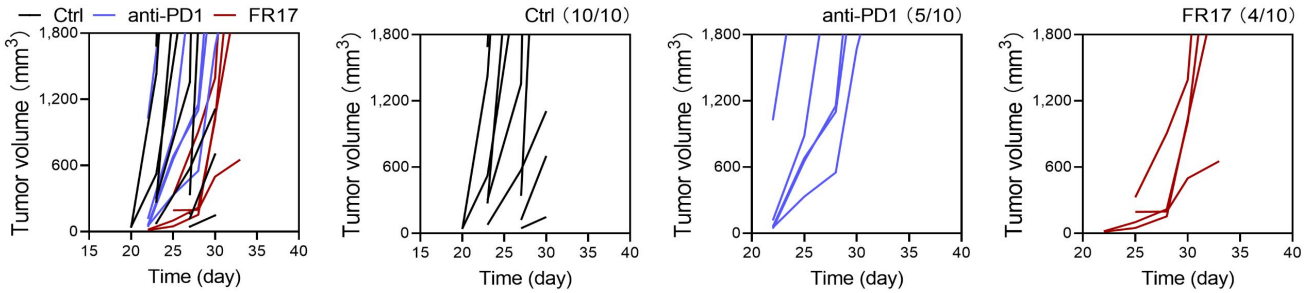

Supplementary Figure 18. Tumor volume curve of the recurrent tumor on the back of mice post-surgery. n = 10 relapses after the surgery in 10 mice for the control group (data points of 1 of the 10 mice is outside the axis limits), n = 5 relapses after the surgery in 10 mice for anti-PD1 group, n = 4 relapses after the surgery in 10 mice for FR17 group.